Reduction of friction in fluid transport: experimental investigation

G.Aguilar*, K. Gasljevic, and E.F. Matthys
Department of Mechanical and Environmental Engineering, University of California Santa Barbara, Santa Barbara CA, 93106, U.S.A.

Recibido el 8 de septiembre de 2006; aceptado el 22 de septiembre de 2006

Drag reduction (*DR*) by the use of polymer and surfactant solutions is by far the most effective drag-reducing technique for turbulent flows (up to 8-fold reduction in friction coefficients is possible on straight pipes). From a fundamental point of view, the study of the *DR* phenomenon offers an opportunity for a better understanding of turbulence in general; from a practical point of view, *DR* can be used to save pumping power. Commercial implementation of drag-reducing fluids has proved successful for oil pipeline transportation, and looks promising for many other applications that are still under investigation, $e.g.$ district heating or cooling systems, hydronic systems in buildings, sewers, irrigation, industrial processes, etc. Our efforts have focused on two main areas: (A) experimental research on momentum and heat transfer of turbulent flows of drag-reducing solutions, and (B) implementation of these solutions in hydronic cooling systems in buildings for energy conservation purposes. This paper describes an overview of the typical experimental research that we conduct in our non-Newtonian fluid mechanics, rheology, and heat transfer laboratory at UCSB.

Keywords: Drag reduction; heat transfer reduction; polymer; surfactant.

La reducción de fricción o de arrastre (*DR*) mediante el uso de soluciones poliméricas o surfactantes es sin duda alguna la técnica de reducción de fricción para flujos turbulentos en tuberías más efectiva (es posible obtener reducciones de hasta un factor de 8 en los coeficientes de fricción en segmentos de tuberías rectas). Desde el punto de vista fundamental, el estudio del fenómeno de *DR* ofrece la oportunidad de comprender mejor flujos turbulentos; desde el punto de vista práctico, la *DR* puede ser usada con propósitos de ahorro en potencia de bombeo. La implementación comercial de estos aditivos se ha llevado a cabo con éxito en el transporte de petróleo, y la investigación necesaria para la implementación de estas soluciones en muchas otras aplicaciones sigue en proceso, p.ej., en sistemas centrales de calefacción y aire acondicionado, sistemas hidrónicos en edificios, desagües, irrigación, procesos industriales, etc. Nuestros esfuerzos se han enfocado en dos áreas principales: (A) investigación experimental sobre la transferencia de momentum y calor para soluciones reductoras de fricción, y (B) la implementación de estas soluciones en sistemas hidrónicos de enfriamiento en edificios con el propósito de ahorrar energía. Este documento pretende dar una noción general de la investigación experimental que llevamos a cabo en nuestro laboratorio de dinámica de fluídos no-Newtonianos, reología, y transferencia de calor en la UCSB.

Descriptores: Reducción de fricción y calor; polímeros; surfactantes.

PACS: 83.60.Yz; 47.50.+d; 47.27.Qb; 44.27.+g

1. Introduction

Since Toms observed the drag reduction phenomenon for the first time in 1948 [1], the possibility of obtaining large reductions in friction and heat transfer in turbulent pipe flows by the use of polymer and surfactant solutions have caught the attention of many researchers. However, despite five decades of research, a full understanding of the fundamentals of this phenomenon is still far from complete. This lack of knowledge is perhaps not so surprising, since the very nature of turbulent flows and the rheology of viscoelastic fluids in much simpler flow fields are ongoing fields of research. Nevertheless, as most of the advances in the studies of the turbulence of Newtonian fluids, progress in the drag reduction field has been made possible due to the development of semi-empirical models that describe various aspects of the transport of momentum and heat. A few examples of these models are shown below.

From a practical point of view, polymer and surfactant drag reduction has been proposed as a viable resource to save energy ($e.g.$ oil transport, ship-drag, sewers, fire-fighting, etc.). In some practical applications it has already produced good results, particularly in those where, besides the reduction in friction, the corresponding reduction in heat is also beneficial, $e.g.$ oil transportation. However, there are still many challenges regarding the appropriate implementation of drag-reducing additives in many other applications, particularly those where the reduction of the heat transfer is not desirable and, therefore, its control is critical for the success of the application ($e.g.$ district cooling and heating systems, hydronic systems in buildings, etc.).

The purpose of this work is to describe briefly some of the problems that are currently studied in our laboratory and their importance in the context of the practical implementation of drag-reducing fluids in real systems, particularly in Heating-Ventilation-and-Air-Conditioning-Systems (HVAC), which constitutes the application we have been most interested in. More details about our work may be found elsewhere [2-5].

2. Experimental Research

2.1. Diameter Effect

The diameter effect problem in the turbulent pipe flow of drag reducing solutions is the additional dependence of the friction coefficient (C_f) on the pipe diameter, which is not fully

taken into account by the Reynolds number (*Re*) as it is for Newtonian fluids. For practical applications, this problem means that it is not possible to predict the C_f on a large diameter pipe given the C_f measurements readily obtained on a small laboratory-scale pipe. Evidently, this problem is particularly significant for large systems, where it is not feasible to perform drag-reducing tests on large pipes and, therefore, smaller laboratory pipes need to be used to scale the problem. With this picture in mind, it is clear that there is a need to develop appropriate scaling correlations.

Previous studies have produced satisfactory models and correlations that have been partially successful in predicting C_f for some polymer solutions [6-16]; however, they are usually too computationally involving and cumbersome to use. Moreover, polymer solutions are generally not used for closed loops because they suffer permanent degradation.

Surfactant solutions—another type of drag-reducing fluids, are better suited for this purpose, since they suffer only temporal degradation when a certain critical wall shear stress ($\tau_{w,cr}$) is exceeded, but recover their drag-reducing ability when the shear stress (τ_w) is reduced. Regarding the diameter effect, some claims have been made that the same scaling procedures usually applicable to polymers are not valid for surfactants [17], and, therefore, with the growing interest in the application of surfactant solutions in real systems, the problem of the diameter effect has to be reevaluated.

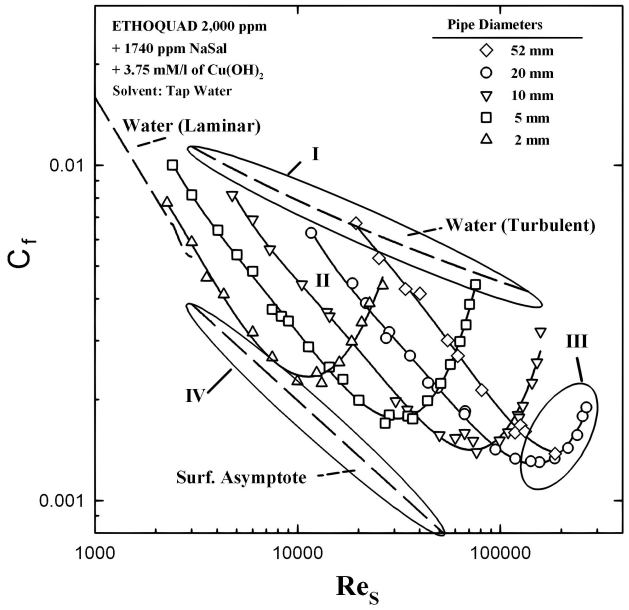

FIGURE 1. Friction coefficients for five pipe diameters (52, 20, 10, 5 and 2 mm) as a function of solvent Reynolds number for an Ethoquad T13/27 solution: 2,000 ppm, plus 1,740 ppm of NaSal, plus 3.75 mM/l of $Cu(OH)_2$. The maximum drag reduction asymptote (MDRA) for surfactants proposed by Zakin *et al.* [21] is shown as a reference. Temp = 20°C. The regions labeled with numbers I, II, III, and IV represent the *vicinity of the onset*, *intermediate*, *supercritical*, and *asymptotic* regions. Note that regions I and IV always correspond to the vicinity of the turbulent Newtonian friction coefficient, and the MDRA, respectively. Regions II and III may vary for different C_f curves. Region III is only marked for the 20 mm diameter pipe data.

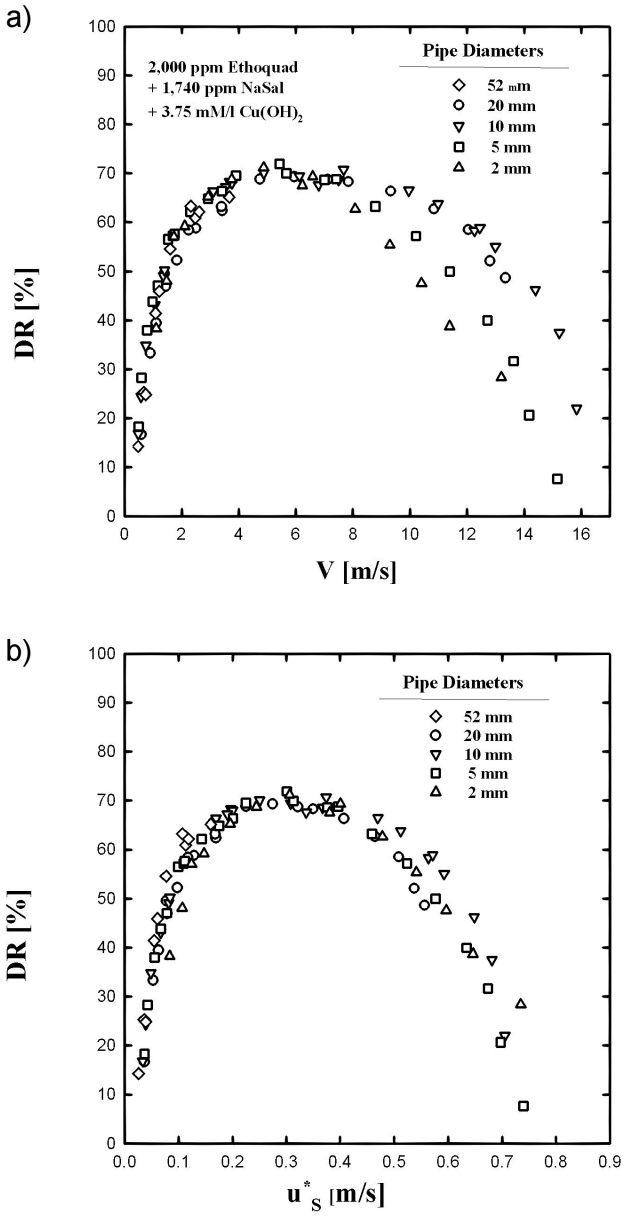

FIGURE 2. a) Drag reduction level (DR) as a function of bulk velocity (V) for the data shown in Fig. 1. b) Drag reduction level (DR) as a function of the solvent shear velocity (u_s^*) for the same data.

Figure 1 shows the C_f measurements for a cationic surfactant solution measured in five pipes of different diameters (2,5,10,20, 52 mm) plotted as a function of the solvent-based *Re*. The surfactant used in this experiment is a tris (2-hydroxys-ethyl) tallowalkyl ammonium acetate (tallowalkyl-N-$(C_2H_4)OH)_3Ac$, from AKZO Chemicals, usually referred to by its trademark: Ethoquad^{TM} T/13-27. This solution consists of 2,000 ppm of surfactant, plus 1740 ppm of Sodium Salicylate (NaSal) used as counterion, and 3.75 mM/l of Copper Hydroxide ($Cu(OH)_2$), which is a compound that

helps reduce the fluid viscosity to a water-like value, without diminishing its drag-reducing ability [33]. The C_f curves corresponding to laminar and turbulent Newtonian flows are also plotted as reference. For clarity, we find it useful to distinguish the different regions that a typical C_f curve goes through. These regions are not strictly defined, and are not necessarily present in all drag-reducing fluids, but they facilitate the discussion in the forthcoming sections. Region I describes the *vicinity of the onset* of drag reduction (*DR*), where the curve shows the first signs of reduction in C_f; region II represents the *intermediate region*, where the C_f curve is progressively reduced as *Re* increases; region III represents the *supercritical region*, where C_f shows an increase after reaching a minimum value, and is usually related to fluid degradation (in this Figure, this region is only marked for the 20 mm diameter pipe data); finally, region IV, is referred to as the *asymptotic region*, where C_f reaches an empirically-determined minimum value, independent of pipe diameter, fluid type, concentration, etc. This region is bounded by the maximum drag-reducing asymptote (MDRA), also shown in Fig. 1 (note that none of the experimental curves shown herein reached the MDRA). In practical terms, it is only meaningful to talk about the diameter effect in the *intermediate region*, since, on the one hand, the *vicinity of the onset* and *asymptotic regions* are bounded by the Newtonian friction coefficient and the MDRA curves, respectively, and these curves are only a function of *Re*. On the other hand, the *supercritical region* denotes fluid degradation, which implies that the properties of the fluid may be different in different diameter pipes at the same *Re*. Clearly this fluid is a good example of a drag-reducing solution with a strong diameter effect.

Figure 2a shows the same data as Fig. 1 plotted according to our proposed scaling procedure [4], $i.e.$, *DR vs.* V. where V stands for bulk velocity, and the drag reduction level, *DR* [%], is used as the dependent variable, which is calculated as:

$$DR[\%] = [(C_{fw} - C_{fs})/C_{fw}] \times 100 \qquad (1)$$

The subscripts w and s refer to water and the solution, respectively. An analogous expression may be used to account for the diameter effect on the heat transfer, where C_f is replaced by the heat transfer coefficient (usually expressed in terms of the Nusselt number, *Nu*, or the Colbourn factor, j_H), and the *DR* is replaced by the heat transfer reduction (*HTR*). Up to about 6 m/sec (*the intermediate region*), all data seem to be very well correlated by one single curve. This correlation is perhaps the simplest and most accurate developed until now (accuracy better than 10% in C_f). Interestingly, besides the success of this correlation for scaling this surfactant solution, it proved to be equally successful when applied to the scaling of various polymer solutions, indicating that, even though polymer and surfactant solutions may show distinctive rheological and drag-reducing characteristics, both kinds of additives may follow the same scaling laws in some cases. For bulk velocities above 6 m/sec (*supercritical region*), the scaling procedure does not work any longer, and smaller diameter pipes show a lower *DR* for the same V. For this region, however, the wall shear stress (or shear velocity $u_s^* = \sqrt{\tau_w/\rho}$) defines better the level of *DR* for a given fluid in all pipes, as illustrated in Fig. 2b. It is known from numerous tests that the temporary degradation of surfactant solutions starts at a critical wall shear stress, $\tau_{w,cr}$, independent of pipe diameter. Therefore, it is reasonable to think that in the *supercritical region* the dominant process would be the fluid degradation, which is primarily dictated by the τ_w.

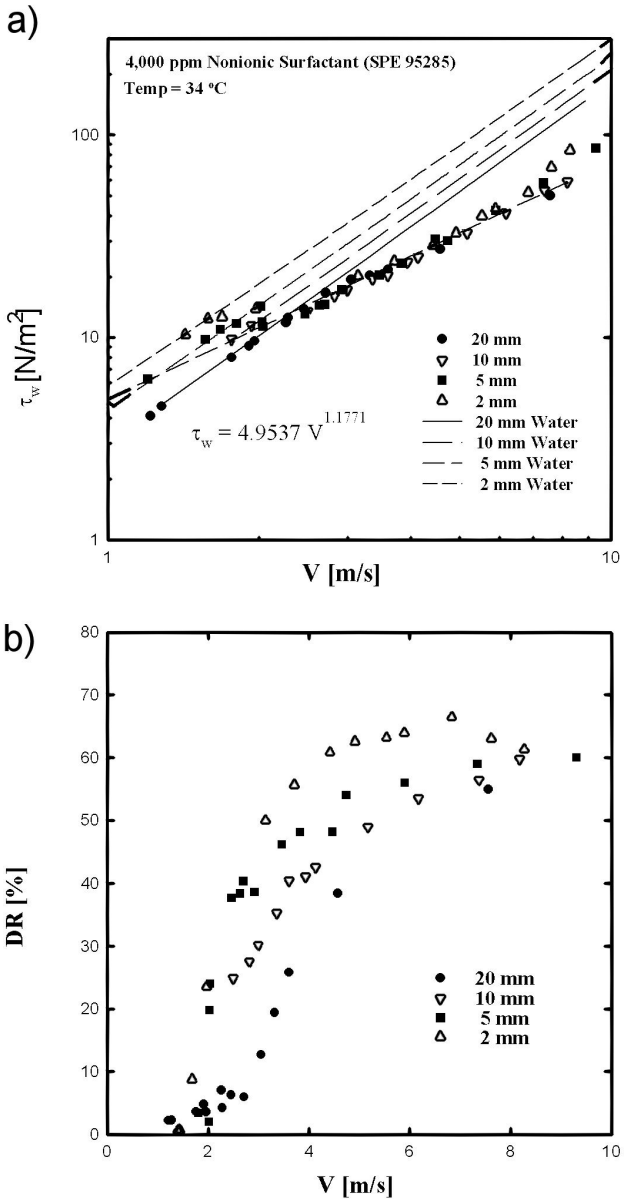

FIGURE 3. a) Wall shear stress as a function of bulk velocity for a 4,000 ppm non-ionic surfactant solution (SPE 95285). The straight lines are the theoretical values corresponding to Newtonian fluids (water). b) Drag reduction level (DR) as a function of bulk velocity (V) for the same data. Note how this choice of variables fails to predict the diameter effect by as much as 30% between the 2 and 20 mm diameter pipes, and how smaller diameter pipes show larger DR than bigger ones.

Figure 3 shows another interesting case, where a different drag-reducing solution does not follow the same scaling correlation as the surfactant solution shown in Fig. 2. These data correspond to a biodegradable non-ionic surfactant solution (SPE 95285 by AKZO Chemicals), which was specifically developed to work in cooling systems, $i.e.$ to have a high drag-reducing efficiency at low temperatures. The presentation in the form of τ_w *vs.* V (top) shows all the data fitting very well on a unique straight line for V between 3 and 8 m/sec (except for a few data points at the highest V which are presumably showing signs of degradation, as mentioned before). The Newtonian curves corresponding to each of the pipe diameters are also shown for reference. This is the procedure that was first introduced as a general scaling correlation applicable to all surfactant solutions [17]. In contrast, the scaling procedure of *DR vs.* V (Fig. 3b) does not work satisfactorily because, for a given velocity, there is up to 30% more *DR* in the 2 mm than in the 20 mm tube.

This evidence seems to suggest that there are at least two distinctive types of drag-reducing behaviors, which are not necessarily related to the nature of the fluid, $i.e.$ polymer or surfactant. To provide information about such different behaviors, we decided to take measurements of the temperature profiles of these fluids, which could presumably allow us to look at the cause for these differences. The results are presented in Sec. 2.4.

2.2. Maximum Drag and Heat Transfer Asymptotes for Surfactant Solutions

Another example of phenomenological models that have been largely developed for polymers, but which have not yet been proven to be equally applicable to surfactants, are the MDRA and the maximum heat transfer reduction asymptotes (MHTRA). The knowledge of these asymptotes is particularly interesting from a practical application standpoint, since they represent the maximum reductions in drag and heat transfer which can be possibly attained by progressively adding an additive to a given solution. Various researchers have proposed MDRA and MHTRA correlations for polymer solutions [18-20], while some others have recognized that the maximum MDRA and MHTRA of surfactants show somewhat larger reductions than those of polymers. Recently, a MDRA was proposed for surfactant solutions [21], but no MHTRA has yet been reported for this kind of fluid. Because of the growing interest in surfactant solutions, we have also tried to develop a MHTRA correlation for surfactants.

Figure 4 shows experimental C_f measurements for various surfactant solutions plotted as a function of the solvent *Re*. Along with our results, a recently proposed MDRA for surfactants [21] is also presented. As may be seen, our measurements show slightly lower values than those predicted by that MDRA, presumably because the solvent viscosity was used for the calculation of *Re*, whereas in reality the fluid may have had a higher viscosity. This is a very important issue because, unlike polymer solutions, surfactant solutions usually have higher shear viscosity, which is in turn highly shear rate dependent and, therefore, makes it more difficult to define the *Re* unequivocally. Bearing this in mind, all our surfactant solutions were intentionally prepared to have water-like viscosity in the range of the *Re* measured (2×10^3 - 80×10^3).

The asymptotic friction coefficient defined by our data in terms of the Prandtl-Karman-type equation can be given as:

$$\frac{1}{\sqrt{C_f}} = 23.9 \log \left(Re\sqrt{C_f} \right) - 40 \qquad (2)$$

approximated by the power law:

$$C_f = 0.18\, Re^{-0.50} \qquad (3)$$

over that range of *Re* and also shown in Fig.4.

Figure 5 represents the results of simultaneous heat transfer measurements of the same fluid in terms of the Colbourn factor (j_H=*Nu*/(*RePr*$^{1/3}$)). As may be seen, the j_H measured for surfactant solutions are lower than those measured for asymptotic polymer solutions [19, 20] (shown as dashed and dotted lines for reference). Provided that the shear viscosity is properly taken into account, a new asymptotic heat transfer correlation applicable to these surfactants and, presumably to a large variety of them, can be well represented by the following power law:

$$j_H = 0.164 Re^{-0.649} \qquad (4)$$

for the range of $12\times10^3 < Re < 80\times10^3$.

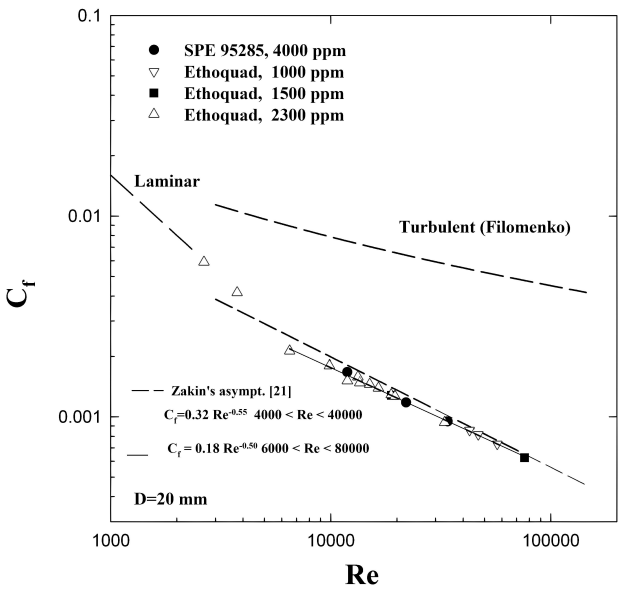

FIGURE 4. Friction coefficient measurements for three cationic surfactant solutions (Ethoquad T13/27): (A) 1000 ppm, plus 870 ppm NaSal, plus 1.5 mM/l $Cu(OH)_2$; (B) 1500 ppm, plus 1300 ppm NaSal, plus 3.0 mM/l $Cu(OH)_2$; (C) 2300 ppm, plus 1740 ppm NaSal, plus 3.75 mM/l $Cu(OH)_2$, and a non-ionic surfactant (SPE 95285): 4000 ppm, plotted as a function of the solvent Reynolds number. Both kinds of surfactants showed water-like viscosity for these experimental conditions.

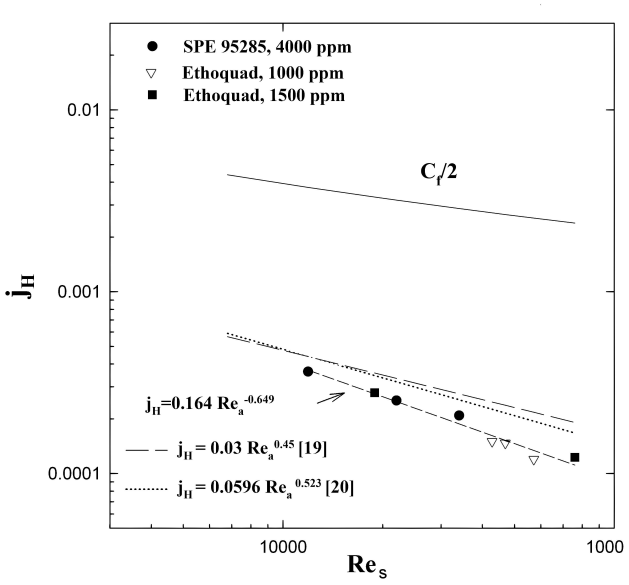

FIGURE 5. Colbourn factor (dimensionless heat transfer coefficient) measured under the same experimental conditions and for the same surfactant solutions shown in Fig. 4.

2.3. Relationship between DR and HTR

Previous studies indicated that the analogies between friction and heat transfer that are valid for Newtonian fluids do not hold for drag-reducing fluids [22-23]. This issue has been explained by the possibility that the turbulent Prandtl number (Pr_t), $i.e.$ the ratio of the eddy diffusivity for momentum (ε_M) to that of heat (ε_H), is somewhat higher than one for these fluids, as opposed to what happens for Newtonian fluids where, $Pr_t \approx 1$. Moreover, it has been reported that, at least under certain circumstances, a decoupling between the *DR* and *HTR* occurs [20,24-25]. The research work we have conducted in this direction is more important from a fundamental point of view than a practical one, but a byproduct of this work is the development of correlations that relate the *DR* to the *HTR*, which allow us to estimate the value of one of them through the measurements of the other. To assess this relationship, we have conducted systematic measurements of C_f and *Nu* for pipes of various diameters, for various fluids, as well as for the different regions of the flow field, $i.e.$ in regions I, II, III, IV, as illustrated in Fig. 1.

To understand better the relationship between the *DR* and *HTR* in the *intermediate regime* (region II), it was considered desirable to examine the effect of the Pr_t on the *HTR*/*DR* ratio. To do this, we first decided to represent the *DR* and *HTR* in terms of slightly different variables, referred to as Turbulence Reduction-Heat (*TRH*), and Turbulence Reduction-Drag (*TRD*), which are defined as:

$$TRD = \frac{(C_{f\,W,T} - C_f)}{(C_{f\,W,T} - C_{f\,W,L})} \times 100;$$

$$TRH = \frac{(Nu_{W,T} - Nu)}{(Nu_{W,T} - Nu_{W,L})} \times 100, \qquad (5)$$

where the subscript T stands for turbulent flow, L for laminar flow and W for solvent (water). The latter definitions are indeed physically more meaningful than those of *DR* and *HTR* since they reflect the degree of turbulence reduction with respect to full laminarization rather than to an artificial fluid with zero viscosity [26]. Secondly, we developed a mathematical model, which allows us to predict the shape of the velocity profile based only on the measurements of TRD. Our model assumes that the velocity profiles are modified with increasing *Re* according to the Virk's 3-layer velocity profile model [18] for drag-reducing fluids. This model consists of a viscous sublayer (similar to that of Newtonian fluids) followed by a buffer or elastic layer. The latter layer grows in thickness as the level of *DR* increases. If this layer extends all the way to the center of the pipe, it leads to *asymptotic DR*, corresponding to the MDRA referred to above. Finally, a third layer is present for intermediate levels of reduction. This is an unaffected portion of the logarithmic layer (but shifted upwards towards the pipe center) and approximately parallel to the Newtonian logarithmic layer (the shift is usually represented by the term ΔB^+). Our model further assumes that the viscous and thermal sublayers remain unaffected, that the buffer layers of the velocity and temperature profiles are of the same thickness, and that the buffer layer slope of the temperature profile varies proportionally to that of the velocity profile (the proportionality constant being given by a constant Pr_t). By doing so, it is possible to compute the variation of *TRH* as a function of the *TRD* for various Pr_t. Details of this model may be found elsewhere [27].

Figure 6 shows the series of curves obtained from our model by performing the computations just described. The values of Pr_t were varied from 1 to 10, assuming a *Re* of

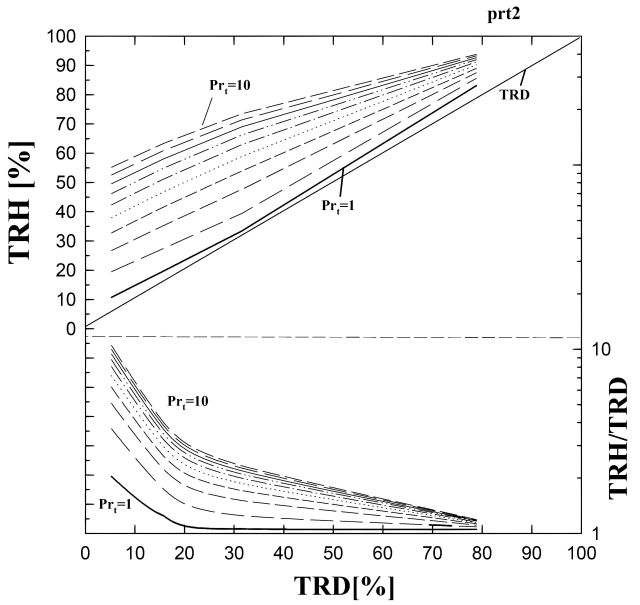

FIGURE 6. TRH *vs.* TRD computed from the mathematical model described in Sec. 2.3 for values of the Pr_t varying from 1 to 10. Re=67000, Pr=6.

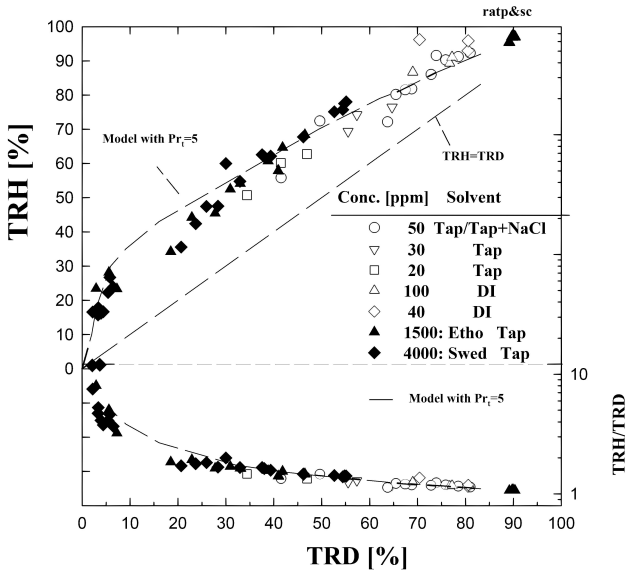

FIGURE 7. TRH *vs.* TRD correlation for various polymer (Polyacrylamide solutions: hollow symbols) and surfactant solutions (Ethoquad and SPE 95285: solid symbols). The dashed line represents the estimated TRH based on a 3-layers temperature profile model analogous to Virk's 3-layers velocity profile model, assuming a constant Pr_t = 5. The TRH/TRD ratio is shown at the bottom for experimental data (symbols) and the model (dashed line).

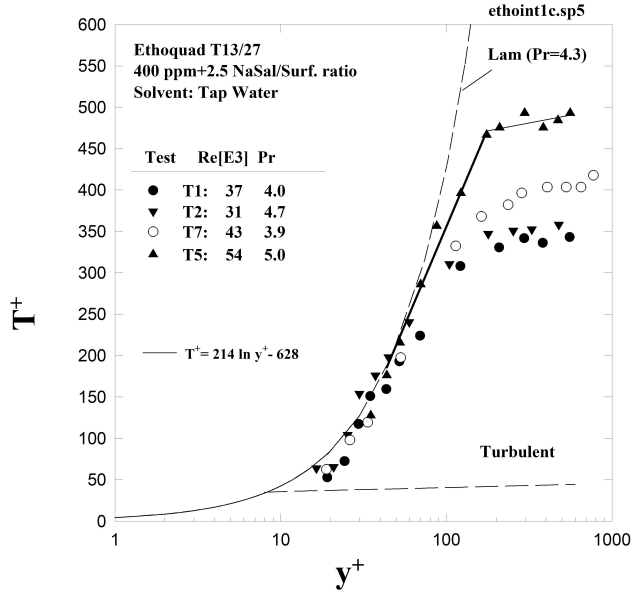

FIGURE 8. Temperature profiles for a 400 ppm Ethoquad solution diluted in tap water plus 2.5 NaSal/Surf. molar ratio as counterion.

67,000 and *Pr* = 6. The top portion of Fig. 6 shows a larger increase in TRH than in TRD at low levels of reduction, which is more noticeable as the value of Pr_t increases. The bottom of Fig. 6 shows the ratio *TRH*/*TRD* also plotted as a function of *TRD* on a logarithmic scale, so that the large variation of this ratio at low levels of reductions can be seen well.

The results of this model were then compared to our data. Figure 7 shows the results of two surfactant solutions (solid symbols) plotted along with polymer solution data (open symbols). Both surfactant solutions shown here had water-like viscosity, and the average *Pr* corresponding to all these fluids was about 6. As may be seen, the reduction in heat is always larger than that in drag, so the *TRH*/*TRD* ratio is always greater than one. However, the *TRH*/*TRD* ratio is larger at low reduction levels and it diminishes as *TRD* increases (see bottom of Fig. 7). In fact, the value of *TRH*/*TRD* at high levels of *TRD* approaches the constant value calculated from the asymptotic conditions presented above; $i.e.$ 1.06 to 1.07, as was expected. It is remarkable to note that, using a unique value of Pr_t of 5 in the model described above, the computed *TRH* (dashed line) fits the measured experimentally *TRH* extremely well. Furthermore, practically the same *TRH*-*TRD* relationship seems to hold for the two types of drag-reducing fluids (polymer and surfactants).

Overall, our results suggest that, although *TRH*/*TRD* seems to be a function of the level of drag-reducing effects (*TRD*), there is indeed a strong coupling between the heat transfer and friction reductions for these fluids through a constant, or approximately constant, Pr_t of about 5.

2.4. Temperature Profile Measurements (Determination of Pr_t)

In order to estimate the local diffusivity coefficients (ε_M and ε_H) and, therefore, to deduce the relationship between momentum and heat transfers on a local level, one needs to provide measurements of the velocity profiles, as well as the mean temperature profiles. Many velocity profile measurements are now available for various solutions of both types of additives (polymers and surfactants) [28-31]. However, there is only one temperature profile reported in the literature that we know of Ref. 32. Given the results of the model computations, and the global measurements that suggest that Pr_t has a value of about 5, we found it necessary to supplement this material by providing the missing part, $i.e.$ additional measurements of the local temperature profiles.

Figure 8 shows four temperature profiles for a 400 ppm Ethoquad solution diluted in tap water plotted in the universal wall coordinates (T^+ *vs.* y^+), where T^+ is the dimensionless wall-to-local temperature difference, and y^+ is the dimensionless distance from the wall. In terms of the scaling procedures, this particular fluid conformed well to the *DR vs.* V correlation (Fig. 2a). As mentioned before, this is the same correlation that applies to many polymer solutions that showed a good fit with the Virk's 3-layer velocity profile model. Therefore, it was expected that the temperature profiles of this fluid would behave analogously to the 3-layer model in the intermediate regime as well. Indeed, in all the profiles, the increase in the *TRH* associated with an increasing velocity is related to an approximately parallel shift in the Newtonian logarithmic layer. Also, the thermal sublayer appears to remain unaffected, and the buffer layer seems to be well represented by a straight line with a slope of approximately 69 (in these coordinates). As a reference, a solid thick

line with the slope of the asymptotic profile is also drawn. The resemblance to the 3-layer model of the velocity profile is noticeable. The resulting Pr_t calculated from the buffer layer slope had a value of about 5, just as the model shown in Fig. 7 predicted.

Figure 9 shows the profiles measured in the intermediate regime for a 2000 ppm non-ionic surfactant (SPE 95285). Evidently, each of these profiles corresponds to a different level of *TRH*. However, note that rather than having one single region close to the wall where most of the interaction takes place, as in the classical 3-layer profiles (the buffer layer), the effect of the *TRH* is spread all the way to the center, even at low levels of reduction. This is what we have referred to as a "*fan-type*" behavior. Note that even small variations at low levels of reduction seem to manifest themselves by significantly affecting the buffer layer slope, and, in contrast with the 3-layer profiles, no plug layer is visible close to the center for any of the profiles.

We have found that this profile pattern can be related to the previously proposed scaling correlation for surfactant solutions, where the τ_w scales with V [17]. Being able to relate the scaling correlations to the local temperature (and velocity) profiles through the measurement of the local diffusivity coefficients allows us to understand more about the effect of these additives in the structure of turbulent flows. For instance, we have shown that the *DR vs.* V correlation is applicable to any fluid showing a 3-layer profile pattern, for which the drag-reducing effect is mostly manifested through the thickening of the buffer layer—a near-wall region. In contrast, the *fan-type* pattern is an indication that the drag-reducing effect may also be manifested throughout the whole cross section of the profile, even at low levels of reduction.

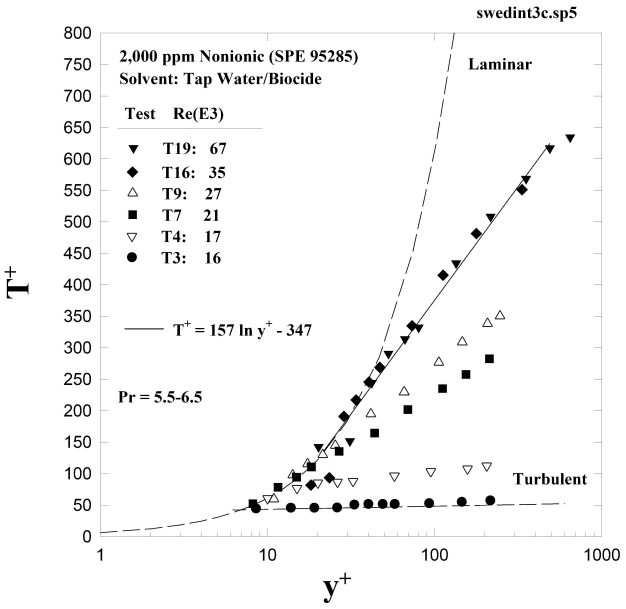

FIGURE 9. Temperature profiles for a 2000 ppm non-ionic surfactant solution diluted in tap water. In this case, the increase in the DR (and HTR) level is reflected as an increase in the slope of the buffer layer, even at low levels of reduction. These are the *Fan-Type* profiles.

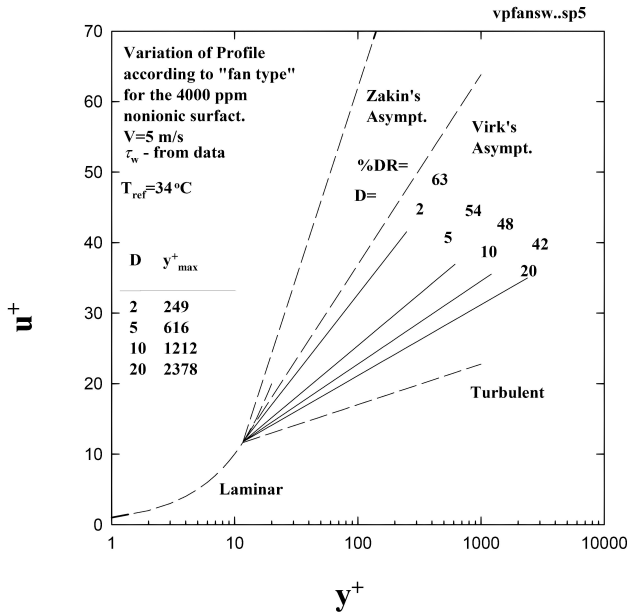

FIGURE 10. Computed variations of the buffer layer slope in different diameter pipes for the fluid which scaled according to the τ_w *vs.*V scaling procedure seen in Fig. 3. The V is arbitrarily kept constant at 5 m/s, and the τ_w is calculated in accordance to the power law correlation obtained from the scaling procedure shown in Fig. 3.

To illustrate the effect of the pipe diameter on the profiles, Fig. 10 shows the estimated velocity profiles for various diameter pipes based on a modified velocity profile model that resembles the *fan-type* pattern just described in Fig. 9. In this model, the viscous sublayer is maintained invariant, the buffer layer slope is allowed to vary to achieve the necessary level of *DR*, and there is no Newtonian logarithmic layer. The bulk velocity V has been arbitrarily chosen to be 5 m/s, and the corresponding τ_w is derived from the power law that resulted from the scaling correlation for the 4,000 ppm nonionic surfactant solution shown in Fig. 3a. As can be seen, the profiles are a function of the pipe diameter, as opposed to the 3-layer profiles where the ΔB^+ shift remained approximately invariant with diameter for a given bulk velocity.

3. Summary and Conclusions

A simple and accurate correlation, *DR vs. V*, was proposed, and it proved to be successful in correlating the diameter effect problem for some polymer and surfactant solutions. With this correlation, we are now able to predict the C_f in a large pipe diameter, given the measurements we can readily perform on smaller pipes in our laboratory.

An MDRA for surfactant solutions was proposed [Eqs. (2)-(3)]. This MDRA allows us to estimate the maximum drag reduction as a function of *Re* only. Also, a new MHTRA for surfactant solutions was proposed (Eq. 4). In this case as well, the complications of higher viscosity solutions were eliminated through the use of solutions with water-like viscosity.

By using a 3-layer velocity and temperature profile model and assuming a similar thickening of the buffer layer, as well as a constant value for the Pr_t, a *TRH-TRD* relationship can be obtained where the *TRH*/*TRD* ratio decreases with an increasing *TRD*. If a constant value of about 5 is chosen for Pr_t, the decreasing *TRH*/*TRD* ratio converges to a value of approximately 1.06, which is the value obtained from the ratio between the experimentally derived asymptotic correlations [Eqs. (3)-(4)]. Moreover, with this value of $Pr_t \approx 5$, good agreement of the model with the polymer and surfactant experimental data is seen throughout the whole *intermediate region* (region II). Furthermore, this estimate is reinforced by the measurement of asymptotic temperature profiles, where $Pr_t = 5$ was also measured.

The surfactant solution that scaled according to the *DR vs. V* correlation (Ethoquad) showed a 3-layer temperature profile. This finding, along with other velocity profile measurements for polymers and surfactants published in the literature, suggests that the aforementioned correlation may be applicable to any drag-reducing solution that conforms to the 3-layer model.

A non-ionic surfactant solution showed a different pattern of temperature profiles: a "*fan-type*". This pattern in turn, corresponds to fluids that scale according to the scaling procedure proposed earlier for surfactant solutions, τ_w *vs.* V [17]. In this case, the drag-reducing effect is spread all the way from the wall to the center, even at low levels of *DR*, contrary to the 3-layer pattern where most of the effect of *DR* is concentrated in the vicinity of the wall.

Acknowledgements

GA wishes to acknowledge the *Universidad Nacional Autónoma de México*, and especially the DGAPA and the IIM for support granted through the scholarship program. The authors wish to acknowledge the financial support of the California Institute for Energy Efficiency (Contract No.4902610 to EFM), and that of the California Energy Commission (Contract No.500-34-022 to EFM).

∗. Corresponding author: Department of Mechanical Engineering, University of California Riverside, Riverside, CA 92521, U.S.A. e-mail: gaguilar@engr.ucr.edu

1. B.A. Toms, In *Proc. of 1st Int. Congress on Rheology*, **2** (Amsterdam: North Holland Pub. Co, 1948) p. 135.
2. K. Gasljevic, *Ph.D. Thesis*, University of California at Santa Barbara, 1995.
3. G. Aguilar, *M.Sc. Thesis*, University of California at Santa Barbara, 1995.
4. Gasljevic, G. Aguilar, and E.F. Matthys, *J. of non-Newtonian Fluid Mechanics* **84** (1999) 131.
5. G. Aguilar, *Ph.D. Thesis*, University of California at Santa Barbara, 1999.
6. N.F. Whitsitt, L.J. Harrington, and H.R. Crawford, Western Co. Report No. DTMB-3, Richardson, TX, AD 677 467, 1968.
7. G. Astarita, G. Greco Jr., and L. Nicodemo, *AIChE J.*, **15** (1969) 564.
8. W.K. Lee, R.C. Vaseleski, and A.B. Metzner, *AIChE J.* **20** (1974) 128.
9. P. Granville, Paper B1 in *Proc. of 2nd Int. Conf. on Drag Reduction*, BHRA Fluid Engineering (Cranfield, England 1977) p. B1-1.
10. P. Granville, Paper C3 in *Proc. of 3rd Int. Conf. on Drag Reduction*, Eds. R.H. Sellin and R.T. Moses (Bristol, England, University of Bristol, 1984) p. C3-1.
11. J.G. Savins and F.A. Seyer, *The Physics of Fluids* **20** (1977) s78.
12. E.F. Matthys and R. Sabersky, *Int. J. Heat and Mass Transfer* **25** (1982) 1343.
13. J.W. Hoyt, *Exp. in Fluids* **11** (1991) 142.
14. J.W. Hoyt and R.H.J. Sellin, *Exp. in Fluids* **15** (1993) 70.
15. H. Usui, T. Itoh, and T. Saeki, *Rheol. Acta* **37** (1998) 122.
16. A. Sood and E. Rhodes, *The Canadian J. of Chem. Eng*. **76** (1998) 11.
17. K. Schmitt, P.O. Brunn, and F. Durst, *Progress and Trends in Rheology II* (1988) p. 249.
18. P.S. Virk, H.S. Mickley, and K.A. Smith, *ASME Journal of Applied Mechanics* **37** (1970) 488.
19. Y.I. Cho and J.P. Hartnett, *Advances in Heat Transfer* (Academic Press, 1982) Vol. 15, p. 60.
20. E.F. Matthys, *J. of Non-Newtonian Fluid Mechanics* **38** (1991) 313.
21. J.L. Zakin, J. Myska, and Z. Chara, *AIChE Journal*, **42** (1996) 3544.
22. T. Mizushina, H. Usui, and T. Yamamoto, *Letters in Heat and Mass Transfer* **2** (1975) 19.
23. K.H. Yoon and A.J. Ghajar, 1987, *Proceedings of the 1987 ASME/AIChE National Heat Transfer Conference*, Pittsburgh, PA. August 9-12.
24. K.S. Ng and J.P. Hartnett, *Studies in Heat Transfer* H.P. Hartnett *et al.* eds. (McGraw-Hill, New York, 1979) p.297.
25. K.S. Ng, Y.I. Cho, and J.P. Hartnett, *AIChE Symposium Series (19 National Heat Transfer Conference)* **76** (1980) 250.
26. K. Gasljevic and E.F. Matthys, *J. of non-Newtonian Fluid Mechanics* **84** (1999) 123.
27. G. Aguilar, K. Gasljevic, and E.F. Matthys, *J. of Heat Transfer (ASME)* **121** (1999) 796.
28. C. Elata, J. Lehrer, and A. Kahanovitz, *Israel Journal of Technology* **4** (1966) 87.

29. M.M. Reischman and W.G. Tiederman, *J. of Fluid Mechanics* **70** (1975) 369.

30. Z. Chara, J.L. Zakin, M. Severs, and J. Myska, *Experiments in Fluids* **16** (1993) 36.

31. H. Beiersdorfer, H.W. Bewersdorff, and A. Gyr, Proc. IUTAM Symp. *On liquid particle interaction and suspensions flow. Grenoble* (1994).

32. Y.E.M. Khabakpasheva and B.V. Perepelitsa, *Heat Transfer-Soviet Research* **5** (1973) 117.

33. Y.T. Hu and E.F. Matthys, *J. of Colloid and Interf. Science* **186** (1997) 352.